Simulation of Land Use Changes in a Coastal Reclaimed Area with Dynamic Shorelines

Jiangfeng She [1,2], Zhongqing Guan [1,2], Fangfang Cai [2], Lijie Pu [2,3], Junzhong Tan [1,2,]* and Tao Chen [1,2]

[1] Jiangsu Provincial Key Laboratory of Geographic Information Science and Technology, Nanjing University, Nanjing 210023, China; gisjf@nju.edu.cn (J.S.); zhongqingguan@gmail.com (Z.G.); chrisplum@smail.nju.edu.cn (T.C.)
[2] School of Geographic and Oceanographic Sciences, Nanjing University, Nanjing 210023, China; cff61212@126.com (F.C.); ljpu@nju.edu.cn (L.P.)
[3] The Key Laboratory of the Coastal Zone Exploitation and Protection, Ministry of Land and Resources, Nanjing 210023, China
* Correspondence: jzhtan@nju.edu.cn; Tel.: +86-25-8968-1296

Abstract: Reclamation is capable of creating abundant land to alleviate the pressure from land shortages in China. Nevertheless, coastal reclamation can lead to severe environmental degradation and landscape fragmentation. It is quite important to monitor land use and cover change (LUCC) in coastal areas, assess coastal wetland change, and predict land use requirements. The siltation of tidal flats will result in the dynamic growth and continuous expansion of coastal areas. Therefore, the process of land change in coastal areas is different from that under the fixed terrestrial boundary condition. Cellular Automata and Multi-Agent System (CA-MAS) models are commonly used to simulate LUCC, and their advantages have been well proven under the fixed boundary condition. In this paper, we propose CA-MAS combined with a shoreline evolution forecast (CA-MAS-SEF) model to simulate the land change in coastal areas. Meanwhile, the newly increased area, because of the dynamic growth of tidal flats, is considered in the simulation process. The simulation results using the improved method are verified, and compared with observed patterns using spatial overlay. In comparison with simulation results that do not consider the expansion of tidal flats, the Kappa coefficient estimated while considering the dynamic growth of tidal flats is improved from 65.9% to 70.5%, which shows that the method presented here can be applied to simulate the LUCC in growing coastal areas.

Keywords: land use and cover change (LUCC); Digital Shoreline Analysis System (DSAS); Cellular Automata (CA); Multi-Agent System (MAS); dynamic growth; tidal flats; reclamation

1. Introduction

Coastal wetlands possess both terrestrial and aquatic characteristics because of their natural tidal frame. They provide valuable ecosystem goods and services and richer species diversity than many other natural environments [1]. Coastal marshes are crucial wetland ecosystems and agricultural land resources. Numerous areas of coastal marshes have been reclaimed in Spain, Germany, Japan, and the Netherlands [2,3]. Reclamation can alleviate the pressure of land loss, but it may cause natural disturbances, such as soil and water pollution, nutrient over-enrichment, and reduction in biodiversity [3],and may bring irreparable damage to ecosystems [4,5]. The spatial patterns of coastal landscapes have become fragmented and heterogeneous under enormous pressure from rapid economic development and population growth [6].

China's coastal wetlands are also threatened due to increasing coastal infrastructure, and the area is expanding through large-scale land reclamations [7,8]. Hundreds of square kilometers are added onto the Chinese mainland each year, as coastlines are extended to a length longer than China's historic "Great Wall" [9]. This "New Great Wall", often built by a hard sea bank, sand pumping, and the introduction of sedimentation-promoting plants (e.g., *Spartina alterniflora*, *Suaeda salsa*), has severely reduced biodiversity and associated ecosystem services in China's coastal area [10]. Meanwhile, local farmers and entrepreneurs also change the coastal ecosystems by individual preferences of land use changes in the coastal wetlands. Both the shoreline dynamics and land use changes are decisive in the provision and protection of coastal wetlands.

It is important to identify viable local management policies for coastal wetlands by assessing the human impacts, as these activities will influence the coastal landscapes, species composition, and functions of the ecosystems [11]. Simulation and projection of the coastal land use changes can help identify the main drivers of wetland conversion and assess the effectiveness of potential response options. There are various land use change models, including Cellular Automata (CA) [12–16], Multi-Agent System (MAS) [17–19], and Expert Models and Hybrid models [20,21]. Among these models, CA and MAS have commonly been used in the field of land use planning and environmental management. CA are grid dynamic models that are discrete in time, space, and state and derive the transitional rules of land use and cover change (LUCC) from empirical data [22]. The powerful complex computing function, high dynamic, and spatial features [23], especially Geographic Information System (GIS) raster data that can be easily embedded in CA simulations [24], make it extremely effective in simulating urban growth and land use evolution [24,25]. MAS models can complete a series of tasks in a complex and dynamic environment, and can adapt to and perceive the change in the environment, features which are widely utilized to simulate the interactions among different activities of individuals with sufficient flexibility [26]. Many scholars have applied the models to land use simulation, and the results indicate that agents can perfectly simulate human behaviors and interactions in the environment [26–28]. Previous studies have used these two models to simulate deforestation, urbanization, and agricultural expansion processes from the local to global scale. Vancheri et al. systematically expatiated the theory of CA-MAS models [29] and applied CA-MAS models to simulate the expansion of Capriasca and Val Colla in the northeastern part of the region of Lugano City [30], proving that it can simulate the complex behavior of the system at the cell scale. Yang et al. presented a case study of Zhangmutou Town, Guangzhou, China, which simulated the urban land expansion during 1988–1993, and obtained the desired simulation results [31]. Increasingly, research studies have proven that the integration of CA with MAS produces better simulation results [32]. CA-MAS models offer the promise of providing both neighborhood influences and interactions between various individuals to the modeling of complex geographic systems [33]. The crucial aspects of CA-MAS models are in discovering the rules and defining behaviors and properties [32,34], which are the only obstacles in their application.

Due to significant reclamation and coastal engineering, the coastline structure changed dramatically in China over the past 70 years [35]. Coastline evolution monitoring and potential change estimation are of great significance for sustainable coastal land resource management and environmental protection [36,37]. Studies have been carried out on coastline change and urban expansion using remote sensing images, which show that most of the coastline change is caused by land reclamation in the Yellow River Delta [38–40], the Yangtze River Delta [41,42], and the Pearl River Delta [37,43]. With development of coastal regions, there is an increasing interest in models that forecast or predict shoreline evolution. Cheryl et al. forecasted the spatial distribution of the coast in Southern California using a Bayesian probabilistic model [44]. Schwarzer et al. applied different methods to predict coastline evolution at different time scales in the Pomeranian Bight, southern Baltic Sea [45]. Lu et al. took the Jiangsu Province coastline as an example, and used the midpoint subdivision interpolation method to explore coastline evolution [46]. However, few models have delineated simulation of LUCC in reclaimed land area under the dynamics of shorelines.

In this paper, we simulated the land use change under the dynamics of shorelines in a typical mudflat depositional zone of Dongtai County, China. The terrestrial area exhibits an increase of the deposition of tidal flats in the study area. With the additional new land, the land use change process is different from other regions. Time series shorelines (1985, 1991, 1997, 2000, 2005, 2010, and 2014) were used to obtain control points to allow calculation of the change rate of the shoreline using the Digital Shoreline Analysis System (DSAS) model. In order to simulate the growth of tidal flats, 62 effective control points were used to simulate the dynamic movement of the coastline. The increase of new tidal flat area was taken into account in the process of land use change. The study included four phases: simulation, validation, prediction, and analysis. The 2010 land use map was simulated using the 2000 land use map as the initial data, which was validated and compared with the land use map in 2010 to evaluate the accuracy of the model. Projections of LUCC in 2020 and 2030 were simulated to predict the land use requirements.

2. Materials and Methods

2.1. Study Area

Dongtai County is located on the east coast of Jiangsu Province, China, and is an important part of the Yangtze River Delta. It includes 85.4 km of coastline, and 1040 km^2 of tidal flats, as of 2013. Due to the deposition of huge amounts of sand transported downstream by the Yangtze River, the coastline is advancing seaward by 150 m every year. Meanwhile, this expansion of the territory toward the sea is occurring at a rate of more than 6 km^2 each year, which makes Dongtai an important source of new land for the country, with large scale reclamation in the coastal area. Moreover, Dongtai is home to the red-crowned crane, whose national nature reserves have been built here on the coastal wetlands.

The study area is located in the coastal reclamation area in the eastern part of Dongtai County (Figure 1). It is an alluvial plain with a typical intertidal mudflat coast [6]. The main land use types are ocean, tidal flat, saltmarsh, aquaculture pond, cropland, river, and built-up land. Reclamation occurred around 1950 in the western part of the study area, and most of the marsh wetlands were reclaimed for aquiculture pond and cropland. Notably, the *Outline of Jiangsu Coastal Reclamation Development Plan* (2010–2020) was released by the State Council of China in 2009, which has greatly accelerated the pace of reclamation in the study area [47].
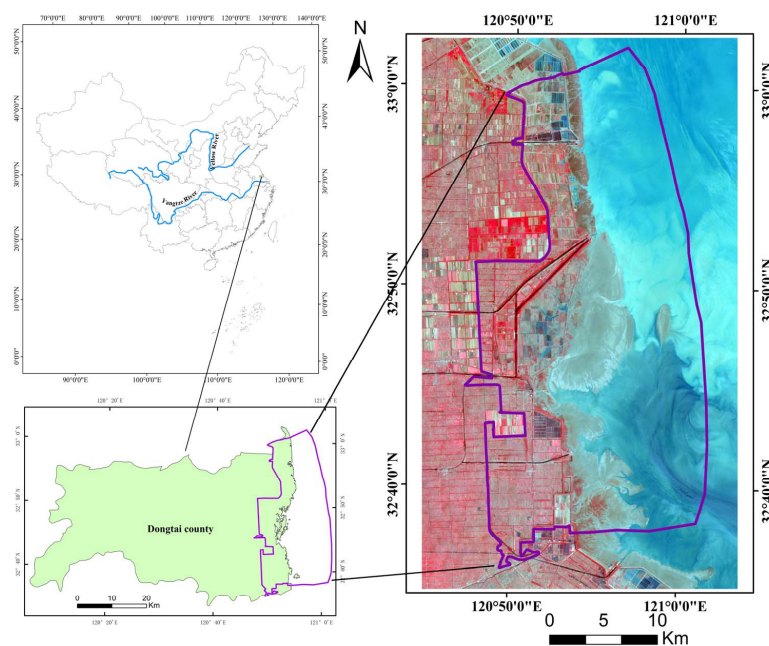

Figure 1. Reclamation area in the eastern part of Dongtai County.

2.2. Data Resources and Processing

The data sets fall into three categories: satellite images, land use data for Jiangsu Province, and river data. Remote sensing data was downloaded from the U.S. Geological Survey (USGS) Earth Resources Observation and Science (EROS) Center [48]. These data were used to obtain time series shorelines and land use maps of the study area, and some of the detailed information is shown in Table 1. In order to reduce the influence of periodic tides on the measurement of the position of the coastline, the imaging time of the remote sensing images was restricted to between 1:30 and 2:30 GMT (Greenwich Mean Time), or 9:30 to 10:30 Beijing time [49]. Taking account of the growth cycle and spectral characteristics of vegetation, the imaging time was restricted to between May and October of each year, which better meets the requirements of the acquisition of shorelines and land use maps. Both Jiangsu land use maps and river data were downloaded from the Yangtze River Delta Science Data Center, the National Earth System Science Data Sharing Infrastructure, and the National Science & Technology Infrastructure of China [50].

All of the satellite images were interpreted using a combination of maximum likelihood classification and manual interpretation [51]. Seven land use types were identified, including ocean, tidal flat, saltmarsh, aquaculture pond, cropland, river, and built-up land. Land use maps from Jiangsu Province and Google Earth were used to check and correct the accuracy of the interpreted images. The classification accuracy of the LUCC types by Kappa coefficients was greater than 0.80, with 0.803, 0.811, 0.821, and 0.805 in 1985, 2000, 2005, and 2010, respectively, which confirmed that the interpretation results better meet the simulation requirements. The study area is rich in artificial rivers, whose widths are about 30 m. The width of these rivers is thus just a single pixel in the remote sensing images; the existing river data was used to help increase the accuracy of the classification of the river.

Table 1. Main parameters and application of remote sensing data.

ID	Sensor	Path/Row	Date	Spatial Resolution (m)	Land Use Classification	Extract the Shoreline
1	TM	119/37	24 September 1985	30	Yes	Yes
2	TM	119/37	23 July 1991	30	No	Yes
3	TM	119/37	20 May 1997	30	No	Yes
4	TM	119/37	13 June 2000	30	Yes	Yes
5	TM	119/37	17 October 2005	30	Yes	Yes
6	TM	119/37	24 May 2010	30	Yes	Yes
7	OLI	119/37	16 March 2014	30	No	Yes

TM is abbreviation of Thematic Mapper, OLI is abbreviation of Operational Land Imager.

2.3. Modeling Land Use Changes under Shoreline Dynamics Based on CA-MAS

2.3.1. Analysis of Shoreline Evolution

The shoreline is dynamic and exposed to never-ending change by the sea, climate, and coastal rivers. The movement of the crust, sediments, and currents reshape beaches, which interact with each other frequently in quite complex ways [43]. Moreover, the impact of reclamation and coastal industry development on the coastal zone is increasing significantly [3]. DSAS is a freely available software application that works conveniently within the Environmental Systems Research Institute's (ESRI) leading GIS software (ArcGIS, Esri, Redlands, CA, USA). DSAS computes the rate of change statistics for a time series of shoreline vector data [52].

After the extraction of the shorelines from remote images (Figure 2), the DSAS was utilized to calculate the rate of coastline change. Firstly, a reference line (1985) was selected; secondly, 157 transects were cast perpendicularly to the baseline at equal intervals of 1 km. The transects crossed the shorelines of each period to obtain the displacement of the coastline between adjacent periods, which were used to calculate the rate of change statistics; finally, the change rate of each transect was calculated by a linear regression method, which is easy to employ, and general computational method [53]. As shown

in Figure 2, shorelines in the middle of study area change constantly without any apparent rule; especially after 2000, the activities of reclamation are more active than ever [54], which resulted in the regression coefficient being very small. In order to get better results, transects that did not meet the requirements were manually deleted or modified, such as: (a) the coastline of the estuary zone is not continuous, and thus we could not consistently get transects; (b) when the regression coefficient of coastline change rate was less than 0.5, it was replaced by artificial end point rates [52,55,56]. After the above-mentioned selections and corrections, 62 effective transects were retained, and the annual growth rate of coastline corresponding to the control points was obtained.
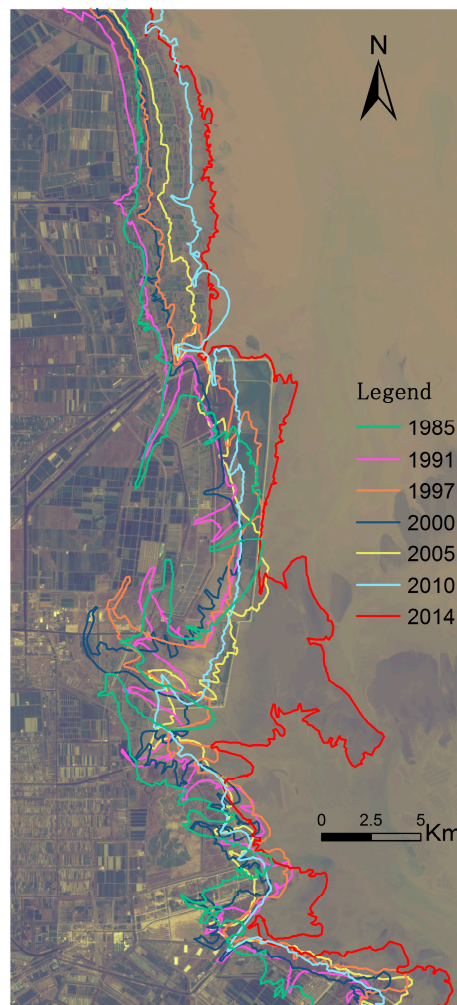

Figure 2. Shorelines extracted from remote images.

2.3.2. Inputs and Parameters in the CA-MAS-SEF Model

The model was designed and implemented in the NetLogo software (Center for Connected Learning and Computer-Based Modeling, Northwestern University, Evanston, IL, USA). NetLogo is a programmable modeling environment for simulating natural and social phenomena [57]. It is particularly well suited for modeling complex systems developing over time and explores the connection between the behavior of individuals and the environment [58,59]. NetLogo provides the ability to load GIS data into a model and saves data as the native NetLogo file format, which greatly improves the convenience for computing in the CA component. The MAS component provides a flexible tool to address the interactions among individuals that can be expressed by "turtles" in NetLogo. The following parts describe the detailed inputs and parameters in implementing this model:

(1) The distance to the ocean map

The initial distance to the ocean map was calculated by land use map in 2000 (Figure 3a), and the value of distance was dynamically updated with expansion of tidal flats every year.

(2) The land "age" map

The land "age" map was calculated by the distance to the ocean map and annual growth rate of coastline (Figure 3b). The equation can be simply described as follows:

$$T_i = D_i / R_{two},\qquad(1)$$

In the equation, T_i is the length of time for location (i) to transform from ocean to land , D_i is the distance of location (i) to the ocean, R_{two} is the mean value of growth rate of two adjacent control points, the *y* coordinate of location (i) is between the *y* coordinate of the two adjacent control points. The value of land "age" increases by one every year.
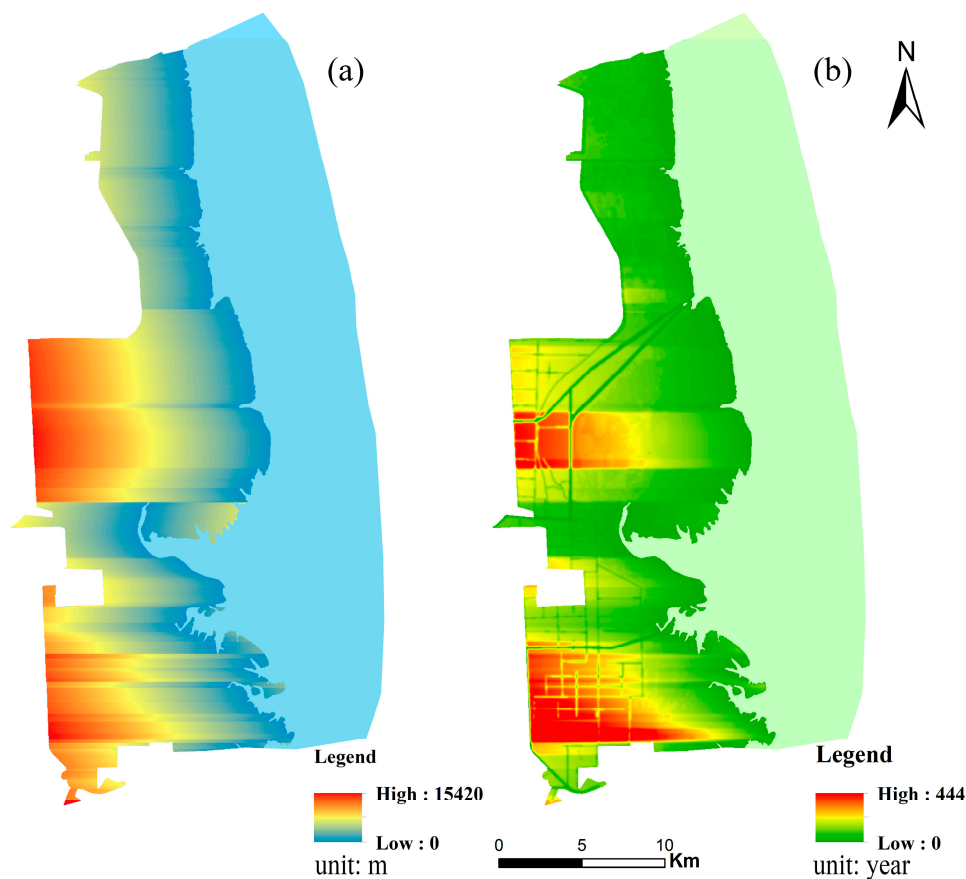

Figure 3. Physical factors: (**a**) The distance to the ocean in 2000; (**b**) The length of time to transform from ocean to land in 2000.

(3) The pond "age" map

The initial pond "age" map was calculated by the land "age" map and minimum pond reclamation "age". The initial value of pond "age" was equal to the value of land "age" minus the minimum pond reclamation "age". The value of pond "age" increases by one every year.

(4) Other important inputs and parameters (shown in Table 2)

Table 2. Other important inputs and parameters.

Name	Type	Explanation
land use map	input	base map, validation map
control points file	input	forecasting shoreline evolution
agent-count	parameter	count of agents, the value was set according to our surveys
agent-accessible-distance	parameter	accessible distance of agent, different agent types have different accessible distances
agent-capacity	parameter	reclaim scope of agent, different agent types have different reclaim scopes
land-distance-ocean	parameter	because of the influence of salinity and other factors, land conversion is limited by distance to the ocean, different land types have different limited distances to the ocean
convert-threshold	parameter	land conversion threshold, different land types have different conversion thresholds, the conversion should strictly adhere to the laws of land use evolution

2.3.3. Simulation of CA-MAS-SEF Model

The CA-MAS-SEF model was implemented to simulate the process of land use change in the coastal area, and the details of the technique are shown in Figure 4. The model consists of three parts: (1) the acquisition of land use data and control points; (2) a definition of the simulation process; and (3) the prediction of future land use by considering the growth of tidal flats.
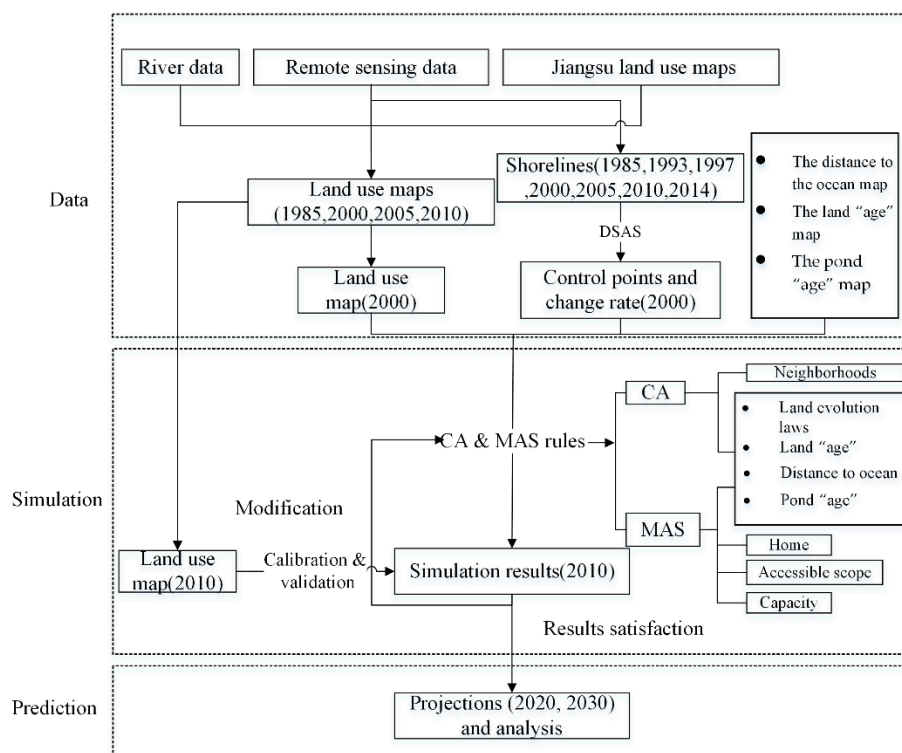

Figure 4. Flowchart of Cellular Automata and Multi-Agent System (CA-MAS) combined with shoreline evolution forecast model.

To better delineate the process of land use change, Figure 5 demonstrates a sequence in the process of land use change. Figure 5a shows the land use pattern at t(a). Deposition results in the accumulation of sediment along or near a coastline. Figure 5b shows new tidal flat area produced at t(b), along with land use change occurring in this process. Tidal flat land transforms to saltmarsh, while aquaculture

pond and cropland appear on saltmarsh land. The change of built-up land can almost be ignored in comparison with cropland and aquaculture pond land, while the river is unchangeable land in our simulation. Figure 5c demonstrates further land change at t(c).
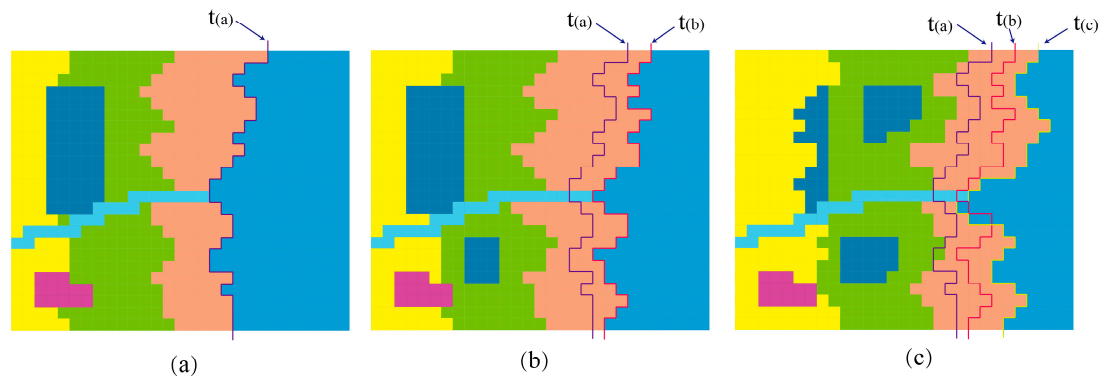

Figure 5. A sequence in the process of land use change: (**a**) Land use pattern at t(a); (**b**) Land use change pattern considering the expansion of tidal flats at t(b); (**c**) Further land use change considering the dynamic growth of tidal flats at t(c).

The extracted control points are mapped onto the land use map and then connected by line to simulate the coastline (Figure 6a). In order to simulate the diverse changes of the coastline, new points are created by stochastic and fractal methods between existing points (Figure 6b,c) [60]. The y coordinate of a new point is equal to the mean y coordinate value of the two nearest points, and the x coordinate is a random number between the x coordinate of the neighbor points. Considering computational efficiency, the number of iterations that can be controlled at the interface should not be too large. The value of iterations is set at seven, which means that $2^7 - 1$ new points are created between any two adjacent control points. The points move seaward along with the coastline every year. Land on the left of the coastline converts to tidal flats, while the right of it is eroded by ocean.
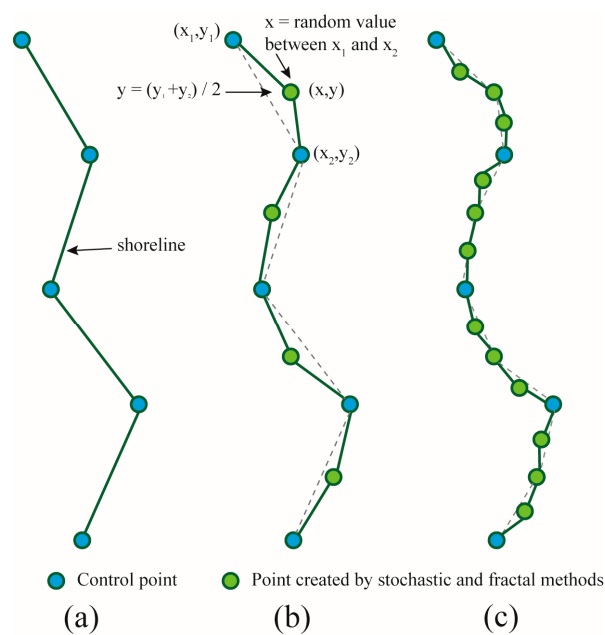

Figure 6. Shoreline simulated by stochastic and fractal methods: (**a**) Control points are connected by a line to simulate the shoreline; (**b**) New random points created between control points; (**c**) More new random points created between points by stochastic and fractal methods.

After land use simulation at t(a), the control points move seaward along with the shoreline at t(b), while newly created points at t(a) disappear after movement of the shoreline (Figure 7a,b). The distance that the control points have moved is equal to the annual growth rate obtained from historical shoreline. The direction of transects obtained from DSAS is not always horizontal, which means that the evolution of the shoreline is complex. To better simulate the evolution, the direction of control points is a random degree between $-\alpha/2$ and $\alpha/2$, where α is set at ten degrees in this study. After the movement of the shoreline, new points are created by stochastic and fractal methods.

According to our surveys and consultations with experts, obvious laws governing land use evolution exist in the study area, and these are tidal flat $\rightarrow$ saltmarsh $\rightarrow$ aquaculture pond $\rightarrow$ cropland $\rightarrow$ built-up land [49,61,62]. The cell state is the land type in CA and the neighborhoods are 3×3 Moore neighborhoods, which means that eight cells have a significant effect on the central cell. Transform rules should strictly adhere to the laws of land use evolution in Table 3. Based on the land use map in 2000, land use patterns in 2010 were predicted.

Many scholars have emphasized the importance of human beings in land use modeling [18]. According to our survey, farmers and entrepreneurs are two types of individuals that have great influence on land use change. Farmers reclaim saltmarshes and convert them to aquaculture ponds. Moreover, saltmarshes and aquaculture ponds are also converted to croplands. Entrepreneurs and farmers have similar behaviors, but the accessible scope and area of reclamation are completely different. In the model, entrepreneur and farmer agents have an initial "home" address, and both of them can only reclaim a certain distance from "home", and convert ecological land to production-orientated land with different capacities. Considering the economic benefits of reclamation, aquaculture ponds should be retained for a certain number of years before being converted to croplands.
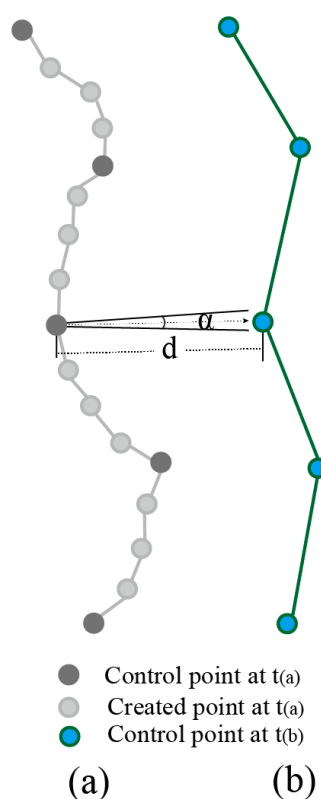

● Control point at t(a)
○ Created point at t(a)
● Control point at t(b)

(a)   (b)

Figure 7. The points move seaward along with the coastline: (**a**) Shoreline at t(a), where points include control points and newly created points at t(a); (**b**) Shoreline at t(b) before new points are created, where control points at t(a) move seaward, and newly created points at t(a) disappear after the movement of the shoreline.

Table 3. Land use evolution laws in the study area.

Original Land Type	Potential Target Land Type
ocean	tidal flat
tidal flat	saltmarsh, aquaculture pond
saltmarsh	aquaculture pond, cropland, built-up land
aquaculture pond	cropland, built-up land
cropland	built-up land

Salinity and moisture in the land determine whether the land can satisfy the conditions of reclamation. However, the change in these is a complicated process with no general rule [63,64], although the proportion of salinity and moisture has a strong relationship with the length of time needed to transform an area from ocean to land. The law of land use types, including the length of time needed to transform an area from ocean to land is summarized in Table 4. Thus, the "age" attribution is set for each cell in the simulation process, and land use change should meet the "age" requirements. The distance to the ocean also has a great influence on salinity and moisture, which affect the land use types as well. Table 4 also shows the law of land use types with the minimum distance to the ocean.

Table 4. The law of land use types including the length of time needed to transform from ocean to land and the distance to the ocean.

Land Use Types	Age (Year)	Minimum Distance to the Coastline (km)
ocean/river	0	0
tidal flat	1–5	0
saltmarsh	5–10	0
aquaculture pond	10–15	6
cropland	more than 15	12
built-up land	more than 15	12

The final decision is made according to a joint change probability, which reflects the combined neighborhood factors and influences of individuals. The model can be simply described as follows [32]:

$$P_i^t = K \times \text{Agent}^t (h,s,c) \times \text{Con}^t(i) \times \Omega^t(i) \times \text{Rand}() \qquad (2)$$

In the equation, P_i^t is the change probability of location (i), K is an adjusted coefficient. Agent^t (h,s,c) denotes the agent mentioned above, where h, s, c represent the agent's home, accessible scope, and capacity, respectively. The function of $\text{Con}^t(i)$ is a combined physical constraint, which includes land evolution laws, land "age", distance to ocean, and pond "age", while $\Omega^t(i)$ is the percentage of change cells in the neighborhood, and Rand() is a random float value between 0 and 1 created by the Monte Carlo method [65]. The final land use conversion is determined by comparison with the conversion threshold.

3. Results

3.1. Model Validation and Comparison

Land use change is a set of complex and non-linear processes faced with numerous uncertainties. Hence, there are no standards for the calibration and validation of land use change models. The validation of a land use change model is not a process of examining whether a model is perfect, but an assessment of how well it performs for the specific purpose [66]. Validation is a crucial part of evaluating the simulation accuracy of models. A common method for validation is to make a comparison between the simulated patterns and the actual observations [67].

The land use map from 2000 was used as the base data to simulate the land use results in 2010 (Figure 8b). As a comparison, the land use change, without considering expansion of the tidal flats, was also acquired (Figure 8a). It can be clearly seen that the tidal flats and saltmarsh lands decrease drastically when the dynamic growth of tidal flats is not considered. Furthermore, the ecological land area does not reach a dynamic balance by comparison with the increasing area of aquaculture ponds and croplands, which may give decision-makers a biased perspective. The Kappa coefficient inspection method is another common method used to compare the consistency of two images [68]. The Kappa coefficient of the results for a simulation that considers the dynamic growth of tidal flats is 70.5%, which is higher than the 65.9% estimated using a simulation with fixed terrestrial boundaries that does not consider the dynamic growth of tidal flats.

In order to better visually compare the simulation results with the land use map, the simulated patterns were spatially overlain on the observed map for the year of the simulation (i.e., 2010) (Figure 9). Most areas have been correctly simulated in the simulation result. At the junction of the land and the sea, many ocean areas are incorrectly simulated into other classes, which also occurs in the tidal flat land. In regard to these incorrectly simulated areas, the model parameters, input data, and uncertainties are likely to have had an adverse influence on the simulation results [69,70]. Furthermore, the process of coastline movement cannot be completely simulated with high accuracy using coastline control points. Change in the built-up land area is not apparent, with only a minor increase. The spatial overlay also visually confirms the good consistency between the simulated and observed patterns in other classes.
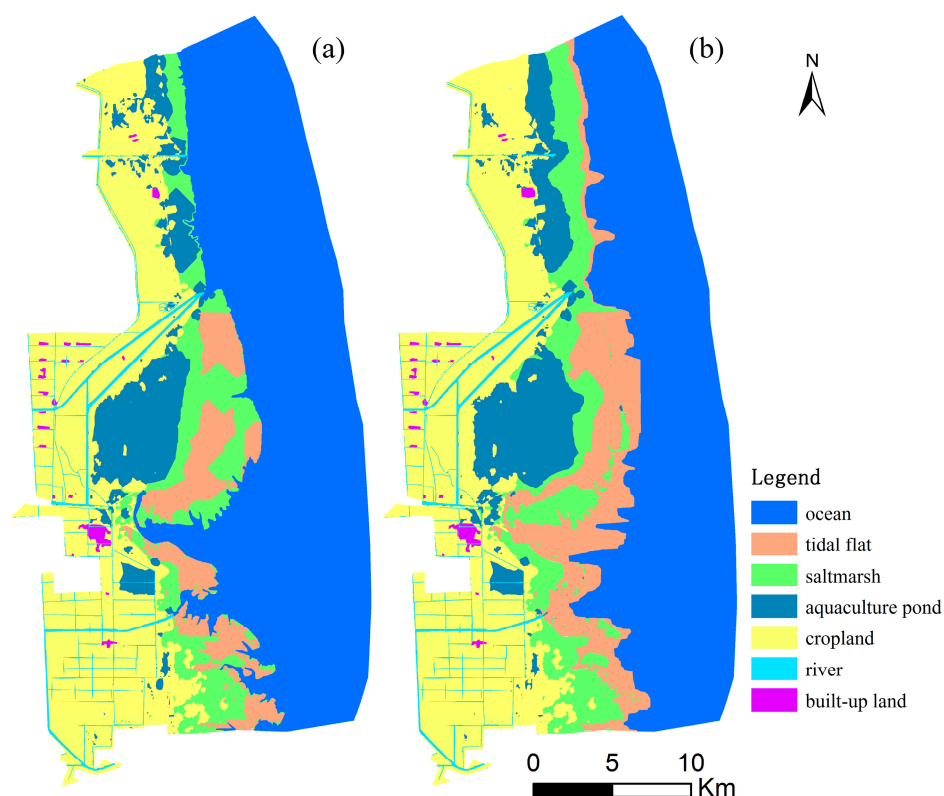

Figure 8. (**a**) Simulated results under fixed terrestrial boundaries; (**b**) Simulated results considering the continuous expansion of the tidal flats.
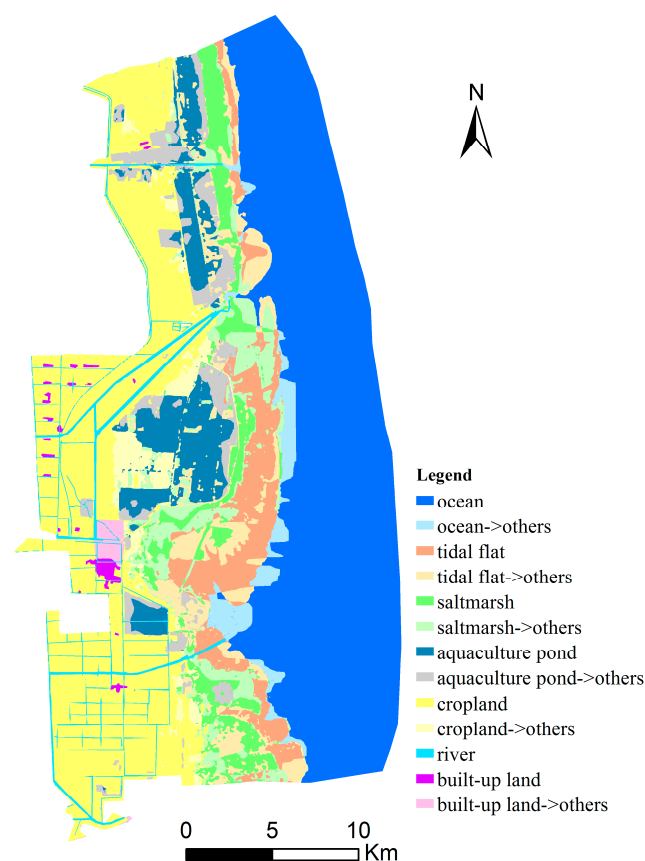
Figure 9. Spatial overlay of simulated results and land use map.

3.2. Potential Future Trends Analysis

The pace of reclamation was relatively slow in the Jiangsu coastal area from 1985 to 2000, but increased significantly after 2000 [54]. Land use change is presented in Figures 10 and 11a. The aquaculture pond and cropland area increased greatly from 1985 to 2010, and intensifying anthropogenic activities accelerated the transformation from ecological to profitable agriculture land. In terms of the statistics of the area (Figure 12), the ocean area continuously decreased from 1985 to 2010, especially after 2000, and an area of 70.9 km^2 was transformed to other land uses from 1985 to 2010. Cropland or agricultural fields increased from 95.7 km^2 in 1985 to 198.5 km^2 in 2010, replacing both saltmarsh and aquaculture pond areas. Aquaculture ponds represented another rapidly increasing land use type, and increased by 67.5 km^2 over 25 years, which was mainly distributed in the north and central parts. Ocean and tidal flats were appropriated for agriculture, aquaculture, and other land uses associated with human demands. The area composed of saltmarshes also decreased, but the decrease was not as significant as the above two types. Due to the addition of new land and the complex conditions of reclamation, the tidal flats area was relatively stable. The increase in built-up land was not obvious.

The predicted spatial patterns in 2020 and 2030 are shown in Figure 11. With the formation of transition areas between terrestrial and marine environments, the aquaculture pond and cropland areas in the north and central parts of the study area are projected to increase rapidly, especially compared with the southern part of the study area. According to the simulation results, the aquaculture area will increase from 70.5 km^2 in 2010 to 83.3 km^2 in 2020, and this value is expected to reach 87.23 km^2 by 2030 (Figure 12). The area of cropland will increase from 198.5 km^2 in 2010 to 214.4 km^2 in 2020, and will further increase to 266.7 km^2 by 2030. Although most of the saltmarsh area and tidal flat area are projected to be converted into profitable land, their combined areas will remain at a relatively stable

value, which are projected to be about 75 km^2 and 80 km^2, respectively. According to the simulations, both land use types maintain a balanced value, which is consistent with the real situation, and proves the reliability of the model. The change in the built-up land area is not obvious. The built-up area only accounts for a small proportion of the total area, and thus shows a minor increase from 2010 to 2030.
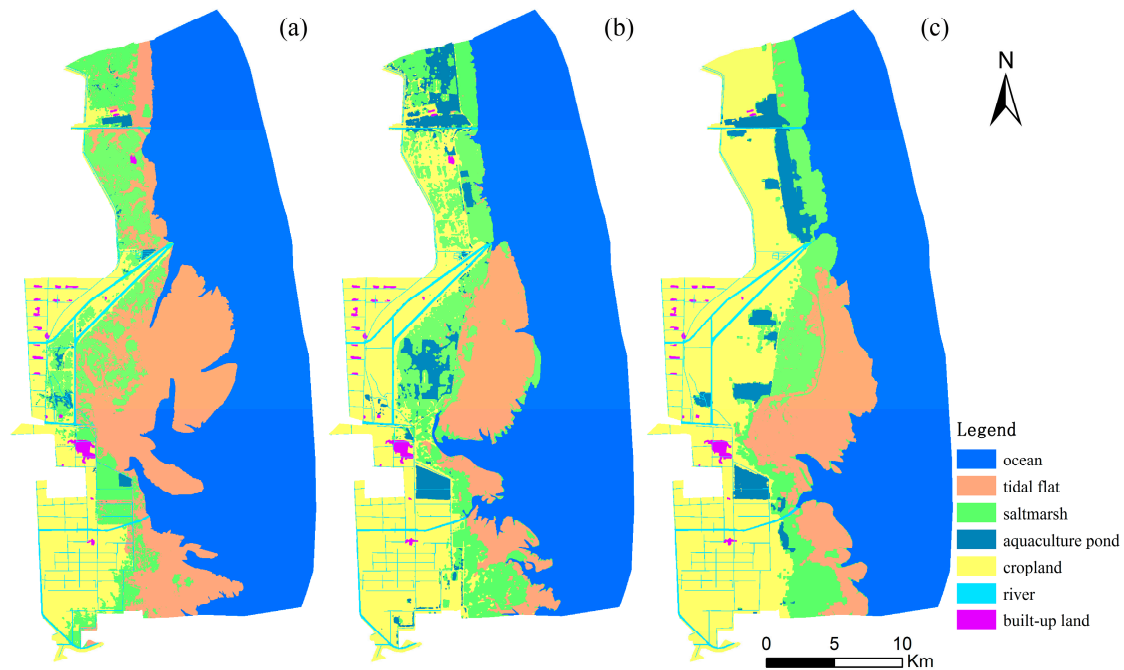

Figure 10. (**a**) Land use map in 1985; (**b**) Land use map in 2000; (**c**) Land use map in 2005.
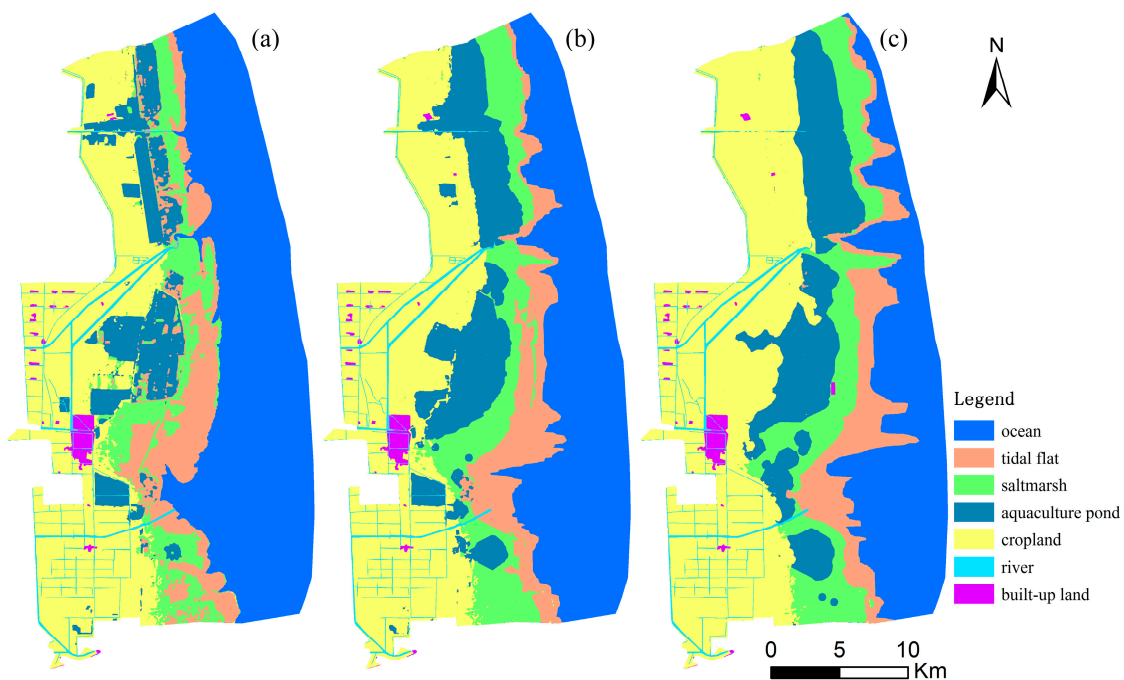

Figure 11. (**a**) Land use map in 2010; (**b**) Simulated results in 2020; (**c**) Simulated results in 2030.
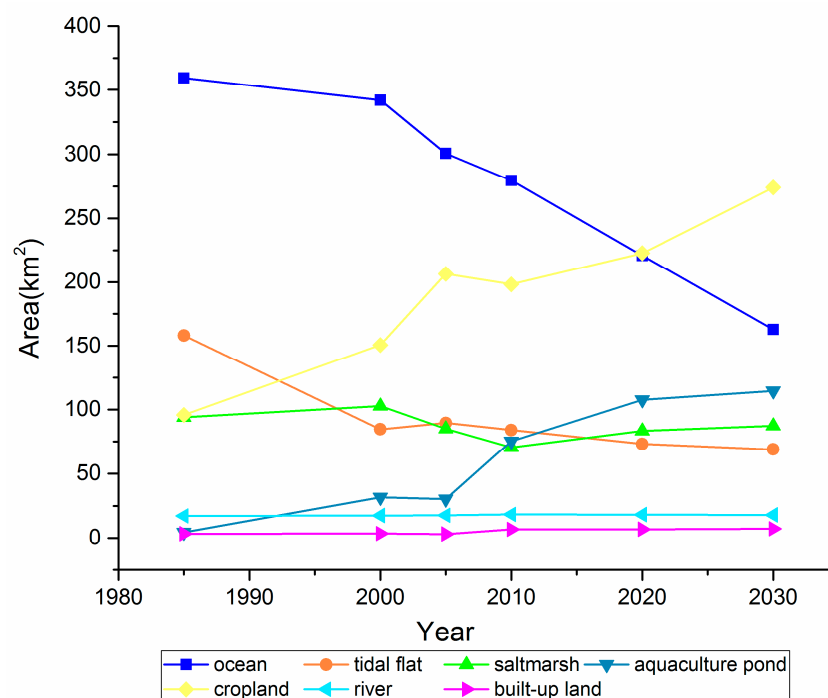
Figure 12. The area statistics of land types in the study area.

4. Discussion

Modeling LUCC is a very challenging task which can be affected by different processes and variables [22]. The same model can generate different outcomes, resulting from the many inherent uncertain factors and the complexity in LUCC simulation [71]. An approach combining CA with GIS promises to deliver a powerful modeling tool, as well as an efficient data handling system. However, CA has a strong sensitivity to cell size [16]. Moreover, the resolution of remote sensing imagery has a great influence on the quality of classification results, and classification error will be passed on to the simulation results, which leads to unavoidable inaccuracy in the simulation results. The real world is a complicated environment, and MAS can simulate interactions among individuals in complex systems. However, the role of human beings is complex. It is difficult to systemically account for all the behaviors of all the individuals as applied to land use. MAS can only simulate the abstract behavior to a certain degree, which will inevitably reduce the accuracy of results. In comparison with cities, the coastal reclamation areas have less social factors that can be considered as spatial variables, but have many more physical constraints to deal with in CA-MAS, which increases the difficulty in applying the existing methods in these areas.

Due to the fluctuating morphological forcing of the waves, tides, and surges, estimation of long-term shoreline movement and its variability remains a difficult open problem [72]. The spatial distribution of land expansion is decided by the shoreline. Accurate prediction of the shoreline influences land use simulation. The annual change rate of the control points was calculated by a regression method. However, the coastline is affected by many factors, especially with the development of reclaimed areas, anthropic activities (e.g., construction of seawalls) change the shoreline, which results in more difficulty in simulating the shoreline with high accuracy. Furthermore, because of the shortage of historical shoreline data, only seven shoreline reference images were obtained, resulting in the need for regression analysis to be conducted more rigorously. In consideration of the computational efficiency, the interval between control points was set about 1 km, but there are many unpredictable variations between adjacent control points. The directions of future shoreline change were controlled by control points, while the direction of transects obtained from DSAS was not horizontal. A random degree was added to the direction of control points, which increases the uncertainty of shoreline

forecast. Consequently, all factors mentioned above contribute to the uncertainty. Coastline has complex shape and self-similarity; when stochastic modeling is used to forecast shoreline evolution, the outcome is not deterministic anymore, but instead has a certain probability of occurrence. In this study, the issue of error in the long-term shoreline forecasts has been neglected, because the uncertainty of random fluctuations in the fractal simulation method is much larger than the error.

The main objective of the present study was to explore the viability of a new model that combines CA-MAS with a shoreline evolution forecast model, which can be used to predict land use change in coastal areas. The method is coarse and still requires further improvements in order to allow analysis of results with greater detail. Although some research indicates that the macrozoobenthos communities can benefit from lower-intensity changes [2], the coastal reclamation area will take more than 30 years to recover to its equilibrium [47,73]. The dynamic interactions between the land and ocean make ecosystems of the coastal wetlands more vulnerable than other regions. It is essential for researchers to pay more attention to the research on LUCC in dynamic growth regions. Further work will focus on delivering a full working model, since the present method was only used to test the operational viability of modeling LUCC in a coastal area. Future research should also cover a more advanced method that would enable the model to simulate more intelligently, in order to help develop a better understanding of environmental protection criteria that should be considered for future coastal planning.

5. Conclusions

The coastal reclamation area is an ecologically fragile area. It is incumbent upon governments to pay attention to the coastal wetland environment by studying land change and predicting future development. This study has demonstrated the utilization of CA-MAS combined with a shoreline evolution forecast model to simulate LUCC changes in a vulnerable, dynamic growth reclamation region. Unlike traditional approaches, the terrestrial area of this study exhibits areal growth through the deposition of tidal flats, which results in an unfixed boundary. The study shows the Kappa coefficient of results for a simulation results that does not consider the dynamic growth of tidal flats is 65.9%, while the Kappa coefficient is improved to 70.5% when estimated using a simulation with unfixed terrestrial boundaries that considers the expansion of tidal flats.

Based on the model, the predictions for 2020 and 2030 reveal several future trends in LUCC in this region. The simulation results show that the area of aquaculture pond and cropland will increase enormously in the next 20 years, with the areas increasing to 87.23 km^2 and 266.66 km^2, respectively, by 2030. Sediment deposition can supply the new tidal flat land, and its area will be maintained at a relatively stable level, which is about 75 km^2. The change in saltmarsh area is also small, the area of which is projected to remain about 80 km^2. However, the spatial location of the saltmarsh moves significantly seaward. The increase in built-up land area is barely apparent. The results emphasize a drastic increase in production-oriented land in the crucial wetlands, and being an ecologically fragile zone, the region should receive appropriate attention. The study findings could provide useful guidance for future exploration of the model and for further research into LUCC in a dynamic growth region. The results should be helpful to the planning and management of the coastal region, as greater efforts are made to develop the area more sustainably.

Author Contributions: Jiangfeng She, Lijie Pu, and Junzhong Tan conceived and designed the experiments; Jiangfeng She and Zhongqing Guan performed the task of data processing, analyzed the results, and wrote the manuscript; Fangfang Cai analyzed the results and edited the manuscript; Tao Chen partially contributed to the editing of the manuscript.

References

1. Provoost, S.; Jones, M.L.M.; Edmondson, S.E. Changes in landscape and vegetation of coastal dunes in northwest Europe: A review. *J. Coast. Conserv.* **2009**, *15*, 207–226. [CrossRef]

2. Cui, B.; He, Q.; Gu, B.; Bai, J.; Liu, X. China's coastal wetlands: Understanding environmental changes and human impacts for management and conservation. *Wetlands* **2016**, *36*, 1–9. [CrossRef]

3. Li, J.; Pu, L.; Zhu, M.; Zhang, J.; Li, P.; Dai, X.; Xu, Y.; Liu, L. Evolution of soil properties following reclamation in coastal areas: A review. *Geoderma* **2014**, *226–227*, 130–139. [CrossRef]

4. Sato, S.i.; Azuma, M. Ecological and paleoecological implications of the rapid increase and decrease of an introduced bivalve *Potamocorbula* sp. After the construction of a reclamation dike in isahaya bay, western Kyushu, Japan. *Palaeogeogr. Palaeoclimatol. Palaeoecol.* **2002**, *185*, 369–378. [CrossRef]

5. Goss-Custard, J.D.; Yates, M.G. Towards predicting the effect of salt-marsh reclamation on feeding bird numbers on the wash. *J. Appl. Ecol.* **1992**, *29*, 330–340. [CrossRef]

6. Ke, C.-Q.; Zhang, D.; Wang, F.-Q.; Chen, S.-X.; Schmullius, C.; Boerner, W.-M.; Wang, H. Analyzing coastal wetland change in the Yancheng national nature reserve, China. *Reg. Environ. Chang.* **2011**, *11*, 161–173. [CrossRef]

7. Sun, Y.; Li, X.; Mander, Ü.; He, Y.; Jia, Y.; Ma, Z.; Guo, W.; Xin, Z. Effect of reclamation time and land use on soil properties in Changjiang River Estuary, China. *Chin. Geogr. Sci.* **2011**, *21*, 403. [CrossRef]

8. Chen, K.; Jiao, J.J. Metal concentrations and mobility in marine sediment and groundwater in coastal reclamation areas: A case study in Shenzhen, China. *Environ. Pollut.* **2008**, *151*, 576–584. [CrossRef] [PubMed]

9. Ma, Z.; Melville, D.S.; Liu, J.; Chen, Y.; Yang, H.; Ren, W.; Zhang, Z.; Piersma, T.; Li, B. Rethinking China's new great wall. *Science* **2014**, *346*, 912–914. [CrossRef] [PubMed]

10. Wang, Y.-S.; Lou, Z.-P.; Sun, C.-C.; Sun, S. Ecological environment changes in Daya Bay, China, from 1982 to 2004. *Mar. Pollut. Bull.* **2008**, *56*, 1871–1879. [CrossRef] [PubMed]

11. Chen, S.-S.; Chen, L.-F.; Liu, Q.-H.; Li, X.; Tan, Q. Remote sensing and GIS-based integrated analysis of coastal changes and their environmental impacts in Lingding Bay, Pearl River Estuary, South China. *Ocean Coast. Manag.* **2005**, *48*, 65–83. [CrossRef]

12. Hegselmann, R. Modeling social dynamics by cellular automata. *Comput. Model. Soc. Process.* **1998**, *23*, 37–64.

13. Schweitzer, C.; Priess, J.A.; Das, S. A generic framework for land-use modelling. *Environ. Model. Softw.* **2011**, *26*, 1052–1055. [CrossRef]

14. Kamusoko, C.; Aniya, M.; Adi, B.; Manjoro, M. Rural sustainability under threat in Zimbabwe–simulation of future land use/cover changes in the Bindura district based on the Markov-cellular automata model. *Appl. Geogr.* **2009**, *29*, 435–447. [CrossRef]

15. Rienow, A.; Goetzke, R. Supporting sleuth—Enhancing a cellular automaton with support vector machines for urban growth modeling. *Comput. Environ. Urban Syst.* **2015**, *49*, 66–81. [CrossRef]

16. Barreira-González, P.; Gómez-Delgado, M.; Aguilera-Benavente, F. From raster to vector cellular automata models: A new approach to simulate urban growth with the help of graph theory. *Comput. Environ. Urban Syst.* **2015**, *54*, 119–131. [CrossRef]

17. Le, Q.B.; Park, S.J.; Vlek, P.L.G.; Cremers, A.B. Land-Use Dynamic Simulator (LUDAS): A Multi-Agent System Model for simulating spatio-temporal dynamics of coupled human–landscape system. I. Structure and theoretical specification. *Ecol. Inform.* **2008**, *3*, 135–153. [CrossRef]

18. Ligtenberg, A.; Bregt, A.K.; van Lammeren, R. Multi-actor-based land use modelling: Spatial planning using agents. *Landsc. Urban Plan.* **2001**, *56*, 21–33. [CrossRef]

19. Berger, T. Agent-based spatial models applied to agriculture: A simulation tool for technology diffusion, resource use changes and policy analysis. *Agric. Econ.* **2001**, *25*, 245–260. [CrossRef]

20. Gilruth, P.T.; Marsh, S.E.; Itami, R. A dynamic spatial model of shifting cultivation in the highlands of Guinea, West Africa. *Ecol. Model.* **1995**, *79*, 179–197. [CrossRef]

21. Yao, F.; Hao, C.; Zhang, J. Simulating urban growth processes by integrating cellular automata model and artificial optimization in Binhai new area of Tianjin, China. *Geocarto Int.* **2015**, *31*, 612–627. [CrossRef]

22. Qiang, Y.; Lam, N.S. Modeling land use and land cover changes in a vulnerable coastal region using artificial neural networks and cellular automata. *Environ. Monit. Assess.* **2015**, *187*, 57. [CrossRef] [PubMed]

23. Crols, T.; White, R.; Uljee, I.; Engelen, G.; Poelmans, L.; Canters, F. A travel time-based variable grid approach for an activity-based cellular automata model. *Int. J. Geogr. Inf. Sci.* **2015**, *29*, 1–25. [CrossRef]
24. García, A.M.; Santé, I.; Boullón, M.; Crecente, R. A comparative analysis of cellular automata models for simulation of small urban areas in Galicia, NW Spain. *Comput. Environ. Urban Syst.* **2012**, *36*, 291–301. [CrossRef]
25. Li, X.; Yeh, A.G.-O. Neural-network-based cellular automata for simulating multiple land use changes using GIS. *Int. J. Geogr. Inf. Sci.* **2002**, *16*, 323–343. [CrossRef]
26. Parker, D.C.; Manson, S.M.; Janssen, M.A.; Hoffmann, M.J.; Deadman, P. Multi-Agent Systems for the simulation of land-use and land-cover change: A review. *Ann. Assoc. Am. Geogr.* **2003**, *93*, 314–337. [CrossRef]
27. Batty, M. Agent-based pedestrian modelling. In *Advanced Spatial Analysis: The CASA Book of GIS*; University College of London: London, UK, 2003; Volume 81.
28. Tsai, Y.; Zia, A.; Koliba, C.; Bucini, G.; Guilbert, J.; Beckage, B. An interactive land use Transition Agent-Based Model (ILUTABM): Endogenizing human-environment interactions in the Western Missisquoi Watershed. *Land Use Policy* **2015**, *49*, 161–176. [CrossRef]
29. Vancheri, A.; Giordano, P.; Andrey, D.; Albeverio, S. Urban growth processes joining cellular automata and multiagent systems. Part 1: Theory and models. *Environ. Plan. B Plan. Des.* **2008**, *35*, 723–739. [CrossRef]
30. Vancheri, A.; Giordano, P.; Andrey, D.; Albeverio, S. Urban growth processes joining cellular automata and multiagent systems. Part 2: Computer simulations. *Environ. Plan. B Plan. Des.* **2008**, *35*, 863–880. [CrossRef]
31. Yang, Q.S.; Xia, L. Integration of Multi-Agent Systems with cellular automata for simulationg urban land expansion. *Chin. Geogr. Sci.* **2007**, *27*, 542–548. (In Chinese)
32. Li, X.; Liu, X. Embedding sustainable development strategies in agent-based models for use as a planning tool. *Int. J. Geogr. Inf. Sci.* **2008**, *22*, 21–45. [CrossRef]
33. Torrens, P.M.; Benenson, I. Geographic automata systems. *Int. J. Geogr. Inf. Sci.* **2005**, *19*, 385–412. [CrossRef]
34. Li, X.; Liu, X. Defining agents' behaviors to simulate complex residential development using multicriteria evaluation. *J. Environ. Manag.* **2007**, *85*, 1063–1075. [CrossRef] [PubMed]
35. Hou, X.; Wu, T.; Hou, W.; Chen, Q.; Wang, Y.; Yu, L. Characteristics of coastline changes in mainland China since the early 1940s. *Sci. China Earth Sci.* **2016**, *59*, 1791–1802. [CrossRef]
36. Serra, P.; Pons, X.; Saurí, D. Land-cover and land-use change in a mediterranean landscape: A spatial analysis of driving forces integrating biophysical and human factors. *Appl. Geogr.* **2008**, *28*, 189–209. [CrossRef]
37. Li, X.; Damen, M.C.J. Coastline change detection with satellite remote sensing for environmental management of the Pearl River Estuary, China. *J. Mar. Syst.* **2010**, *82*, S54–S61. [CrossRef]
38. Murray, N.J.; Clemens, R.S.; Phinn, S.R.; Possingham, H.P.; Fuller, R.A. Tracking the rapid loss of tidal wetlands in the Yellow Sea. *Front. Ecol. Environ.* **2014**, *12*, 267–272. [CrossRef]
39. Ottinger, M.; Kuenzer, C.; Liu, G.; Wang, S.; Dech, S. Monitoring land cover dynamics in the Yellow River Delta from 1995 to 2010 based on landsat 5 tm. *Appl. Geogr.* **2013**, *44*, 53–68. [CrossRef]
40. Chang, J.; Liu, G.; Liu, Q. Dynamic monitoring of coastline in the Yellow River Delta by remote sensing. *Geo-Inf. Sci.* **2004**, *1*, 020.
41. Zhao, B.; Kreuter, U.; Li, B.; Ma, Z.; Chen, J.; Nakagoshi, N. An ecosystem service value assessment of land-use change on Chongming Island, China. *Land Use Policy* **2004**, *21*, 139–148. [CrossRef]
42. Ding, H.; Wang, R.-C.; Wu, J.-P.; Zhou, B.; Shin, Z.; Ding, L.-X. Quantifying land use change in Zhejiang coastal region, China using multi-temporal landsat TM/ETM+ images. *Pedosphere* **2007**, *17*, 712–720. [CrossRef]
43. Ramalho, R.S.; Quartau, R.; Trenhaile, A.S.; Mitchell, N.C.; Woodroffe, C.D.; Ávila, S.P. Coastal evolution on volcanic oceanic islands: A complex interplay between volcanism, erosion, sedimentation, sea-level change and biogenic production. *Earth Sci. Rev.* **2013**, *127*, 140–170. [CrossRef]
44. Hapke, C.; Plant, N. Predicting coastal cliff erosion using a bayesian probabilistic model. *Mar. Geol.* **2010**, *278*, 140–149. [CrossRef]
45. Schwarzer, K.; Diesing, M.; Larson, M.; Niedermeyer, R.O.; Schumacher, W.; Furmanczyk, K. Coastline evolution at different time scales—Examples from the pomeranian bight, Southern Baltic Sea. *Mar. Geol.* **2003**, *194*, 79–101. [CrossRef]
46. Lu, J.; Wang, J.; Zhu, X.; Lv, G. Coastline fractal simulation method and its application—Taking the Jiangsu coastline as an example. *J. Oceanogr. Huanghe Bohai* **2002**, *20*, 47–52. (In Chinese)

47. Xu, C.; Pu, L.; Zhu, M.; Li, J.; Chen, X.; Wang, X.; Xie, X. Ecological security and ecosystem services in response to land use change in the coastal area of Jiangsu, China. *Sustainability* **2016**, *8*, 816. [CrossRef]

48. U.S. Geological Survey (USGS) Earth Resources Observation and Science (EROS) Center. Available online: http://earthexplorer.usgs.gov/ (accessed on 15 November 2016).

49. Li, J.; Pu, L.; Xu, C.; Chen, X.; Zhang, Y.; Cai, F. The changes and dynamics of coastal wetlands and reclamation areas in central Jiangsu from 1977 to 2014. *Acta Geogr. Sin.* **2015**, 17–28. (In Chinese)

50. Yangtze River Delta Science Data Center, National Earth System Science Data Sharing Infrastructure, National Science & Technology Infrastructure of China. Available online: http://nnu.geodata.cn:8008/ (accessed on 15 November 2016). (In Chinese)

51. Foody, G.M.; Campbell, N.A.; Trodd, N.M.; Wood, T.F. Derivation and applications of probabilistic measures of class membership from the maximum-likelihood classification. *Photogramm. Eng. Remote Sens.* **1992**, *58*, 1335–1341.

52. Thieler, E.R.; Himmelstoss, E.A.; Zichichi, J.L.; Ergul, A. Digital Shoreline Analysis System (DSAS) Version 4.0—An Arcgis Extension for Calculating Shoreline Change. Available online: https://woodshole.er.usgs.gov/project-pages/DSAS/version4/ (accessed on 11 March 2017).

53. Dolan, R.; Fenster, M.S.; Holme, S.J. Temporal analysis of shoreline recession and accretion. *J. Coast. Res.* **1991**, *7*, 723–744.

54. Zhao, S.S.; Liu, Y.X.; Li, M.C.; Sun, C.; Zhou, M.X.; Zhang, H.X. Analysis of Jiangsu tidal flats reclamation from 1974 to 2012 using remote sensing. *China Ocean Eng.* **2015**, *29*, 143–154. [CrossRef]

55. Moussaid, J.; Fora, A.A.; Zourarah, B.; Maanan, M.; Maanan, M. Using automatic computation to analyze the rate of shoreline change on the Kenitra Coast, Morocco. *Ocean Eng.* **2015**, *102*, 71–77. [CrossRef]

56. Addo, K.A.; Walkden, M.; Mills, J.P.T. Detection, measurement and prediction of shoreline recession in Accra, Ghana. *ISPRS J.Photogramm. Remote Sens.* **2008**, *63*, 543–558. [CrossRef]

57. Wilensky, U. *Netlogo*; Center for Connected Learning and Computer-Based Modeling, Northwestern University: Evanston, IL, USA, 1999; Available online: http://ccl.Northwestern.Edu/netlogo/ (accessed on 17 February 2017).

58. Shen, Z.; Yao, X.A.; Kawakami, M.; Chen, P.; Koujin, M. Integration of MAS and GIS using Netlogo. In *Geospatial Techniques in Urban Planning*; Springer: Berlin/Heidelberg, Germany, 2012; pp. 369–388.

59. Tisue, S.; Wilensky, U. Netlogo: A Simple Environment for Modeling Complexity. In Proceeedings of the International Conference on Complex Systems, Boston, MA, USA, 16–21 May 2004; pp. 16–21.

60. Zhu, X.; Cai, Y.; Yang, X. On fractal dimensions of China's coastlines. *Math. Geol.* **2004**, *36*, 447–461.

61. Zhai, K.; Liu, M.-S.; Xu, C.; Cui, L.-J.; Xu, H.-Q. Land use/cover change in Yancheng Coastal Wetland. *Chin. J. Ecol.* **2009**, *28*, 1081–1086. (In Chinese)

62. Xu, Y.; Pu, L. The variation of land use pattern in tidal flat reclamation zones in Jiangsu coastal area: A case study of Rudong county of Jiangsu Province. *J. Nat. Resour.* **2014**, *29*, 643–652. (In Chinese)

63. Li, P.; Pu, L.-J.; Zhu, M.; Xu, Y.; Xie, T.; Zhang, R.; Zhang, J.; Sun, Y. Characteristics of soil profile salt in tidal flats under different reclamation years in Jiangsu province. *Resour. Sci.* **2013**, *35*, 764–772. (In Chinese)

64. Liu, G.; Yang, J.; Jiang, Y. Salinity characters of soils and groundwater in typical coastal area in Jiangsu province. *China Acad. J. Electr. Publ. House* **2005**, *37*, 163–168. (In Chinese)

65. Wu, F.; Webster, C.J. Simulation of land development through the integration of cellular automata and multicriteria evaluation. *Environ. Plan. B Plan. Des.* **1998**, *25*, 103–126. [CrossRef]

66. van Vliet, J.; Bregt, A.K.; Brown, D.G.; van Delden, H.; Heckbert, S.; Verburg, P.H. A review of current calibration and validation practices in land-change modeling. *Environ. Model. Softw.* **2016**, *82*, 174–182. [CrossRef]

67. Ward, D.P.; Murray, A.T.; Phinn, S.R. A stochastically constrained cellular model of urban growth. *Comput. Environ. Urban Syst.* **2000**, *24*, 539–558. [CrossRef]

68. Yang, J.; Chen, F.; Xi, J.; Xie, P.; Li, C. A multitarget land use change simulation model based on cellular automata and its application. *Abstr. Appl. Anal.* **2014**, *2014*, 375389. [CrossRef]

69. Verburg, P.H.; Tabeau, A.; Hatna, E. Assessing spatial uncertainties of land allocation using a scenario approach and sensitivity analysis: A study for land use in Europe. *J. Environ. Manag.* **2013**, *127*, S132–S144. [CrossRef] [PubMed]

70. Li, X.; Liu, X.; Yu, L. A systematic sensitivity analysis of constrained cellular automata model for urban growth simulation based on different transition rules. *Int. J. Geogr. Inf. Sci.* **2014**, *28*, 1317–1335. [CrossRef]

71. Brown, D.G.; Page, S.; Riolo, R.; Zellner, M.; Rand, W. Path dependence and the validation of agent-based spatial models of land use. *Int. J. Geogr. Inf. Sci.* **2005**, *19*, 153–174. [CrossRef]

72. Reeve, D.E.; Spivack, M. Evolution of shoreline position moments. *Coast. Eng.* **2004**, *51*, 661–673. [CrossRef]

73. Zhang, R.; Pu, L.; Li, J.; Zhang, J.; Xu, Y. Landscape ecological security response to land use change in the Tidal Flat Reclamation Zone, China. *Environ. Monit. Assess.* **2016**, *188*, 1. [CrossRef] [PubMed]